

NMR resolution enhancement and homonuclear decoupling using non-uniform weighted sampling

Christopher A. Waudby^{1,*} and John Christodoulou¹

¹Institute of Structural and Molecular Biology, University College London and Birkbeck College, London UK

*c.waudby@ucl.ac.uk

ABSTRACT

Non-uniform weighted sampling (NUWS) is a simple method for multi-dimensional NMR spectroscopy in which window functions are applied during acquisition by sampling varying numbers of scans across indirect dimensions. While NUWS was previously shown to provide modest increases in sensitivity, here we describe a complementary application to enhance spectral resolution by increasing the sampling of later points of the time domain signal. Moreover, by combining NUWS with carefully constructed apodization functions signal envelopes can be modulated in an arbitrary manner while retaining a uniform noise level, permitting further signal manipulations such as linear prediction and non-uniform sampling (NUS). We leverage this to develop a combined NUWS-NUS scheme for broadband homonuclear decoupling, with substantially increased sensitivity in comparison to constant time experiments.

Resonance line broadening due to transverse relaxation is one of the key limitations to precise determination of multiple coupling constants in small molecules, or to the characterization of large biomolecules by NMR spectroscopy, due to the inability to satisfactorily resolve overlapping cross-peaks from multiple residues or spin systems. Many approaches have been developed to circumvent this problem including increasing magnetic field strengths¹; non-uniform sampling (NUS) and spectral aliasing^{2,3}; a variety of isotopic labelling schemes employing deuteration to reduce transverse relaxation rates⁴; transverse relaxation optimized (TROSY) experiments^{5,6}; or, most simply, the use of window functions (apodization) to enhance resolution (at the expense of sensitivity).

A second common problem in NMR spectroscopy is homonuclear decoupling of adjacent ¹³C spins, for example in ¹H,¹³C correlation spectra of uniformly ¹³C-labelled biomolecules. Such couplings give rise to a cosine modulation, $\cos(\pi Jt)$, in the free-induction decay (FID), which leads to broadening or a resolved multiplet structure. As for molecular weight, a variety of approaches have been developed to address this problem: isotopic labelling schemes that eliminate adjacent ¹³C nuclei^{4,7,8}; band selective decoupling (although this is only effective for a subset of residues)⁹; virtual decoupling by computational deconvolution¹⁰; and constant time evolution, which while effective entails a substantial reduction in sensitivity¹¹.

Here, we show that non-uniform weighted sampling (NUWS), coupled to NUS reconstruction algorithms, can provide a new solution to both problems. NUWS is an acquisition scheme originally developed to improve experimental sensitivity, by weighting acquisition in indirect dimensions towards early points in free induction decay (FID) signals, at which signal to noise levels are higher¹². Such non-uniform weighting has the effect of applying a window function directly, rather than through apodization, and it can be proved that window functions applied in this manner provide a 10–20% increase in experimental sensitivity (depending on the window function) compared to identical apodization of uniformly sampled data¹³. These sensitivity gains can further accumulate in ≥ 3 D experiments¹⁴. The approach is particularly useful with combined with longitudinal relaxation-optimised experiments such as SOFAST or BEST experiments^{15–17}, the fast repetition rates of which allow a large number of scans to be acquired following a smoothly varying weighting scheme¹³, and this has since been applied to

highly sensitivity-limited studies of co-translational folding and chaperone interactions in ribosome–nascent chain complexes¹⁸.

We first describe the application of NUWS to enhance the resolution in indirect dimensions of multidimensional NMR experiments, through the acquisition of an exponentially increasing number of scans to counteract the relaxation of signals along the indirect acquisition time (Fig. 1A). We consider the application of a window function, $w(t) = e^{\Gamma t}$, to a signal with envelope $s(t) = e^{-Rt}$, acquired with sampling weights, $n(t) = \lceil e^{\alpha \Gamma t} \rceil$, where $\lceil \dots \rceil$ indicates rounding to the nearest integer. These weights indicate the number of repetitions of the minimum phase cycle to be acquired at a given time point. The case $\alpha = 0$ corresponds to uniform sampling (US), while $\alpha = 1$ or 2 corresponds to NUWS and will be considered in more detail below. In all cases, acquired data are multiplied by an apodization function, $h(t)$:

$$h(t) = w(t)/n(t) = e^{\Gamma t} / \lceil e^{\alpha \Gamma t} \rceil \approx e^{(1-\alpha)\Gamma t} \quad (1)$$

to ensure that the final signal envelopes, $y(t)$, are exactly modulated by the desired window function, $w(t)$:

$$y(t) = s(t)n(t)h(t) = e^{-(R-\Gamma)t} \quad (2)$$

The noise, relative to the noise σ_0 obtained from a single acquisition of the minimal phase cycle, increases as the square root of the number of scans:

$$\sigma(t) = \sigma_0 n(t)^{1/2} h(t) = \sigma_0 \lceil e^{\alpha \Gamma t} \rceil^{1/2} e^{(1-\alpha)\Gamma t} \approx \sigma_0 e^{(1-\alpha/2)\Gamma t} \quad (3)$$

For a maximum acquisition time T , the mean sampling weight is (approximately, assuming a large number of increments and allowing non-integer sampling weights):

$$\bar{n} = \frac{e^{\alpha \Gamma T} - 1}{\alpha \Gamma T} \quad (4)$$

Following our previous approach¹³, we may now show that the sensitivity for a total number of scans N , distributed according to the sampling density $n(t)$, is:

$$\text{SNR} = \frac{N^{1/2}}{\sigma_0} \frac{\alpha(2-\alpha)}{\lceil e^{\alpha \Gamma T} - 1 \rceil \lceil e^{(2-\alpha)\Gamma T} - 1 \rceil} \frac{e^{(\Gamma-R)T} - 1}{\Gamma - R} \quad (5)$$

This expression has a maximum when $\alpha = 1$, and is symmetric about this point. This corresponds to ‘conventional’ NUWS (Fig. 1A, green), in which the resolution enhancement is applied directly through the number of scans, and the apodization function $h(t) \approx 1$ (the approximation reflecting compensation for the integer sampling weights). The gain in sensitivity per unit time, relative to uniform sampling, may be calculated from Eq. 5 and is dependant only on the product ΓT :

$$\text{relative sensitivity} = \sqrt{\frac{\Gamma T}{2} \coth \frac{\Gamma T}{2}} \quad (6)$$

This expression is plotted in Fig. 1B. From this, we anticipate that useful sensitivity increases may be obtained, for example, 44% in the case of 40 s^{-1} resolution enhancement and 100 ms acquisition time used in the example below ($\Gamma T = 4$). However, due to the increasing number of scans at long acquisition times, the noise level will also increase exponentially during the FID, which may lead to a degradation in the quality of the spectrum baseline or the ability to extend the FID through linear prediction.

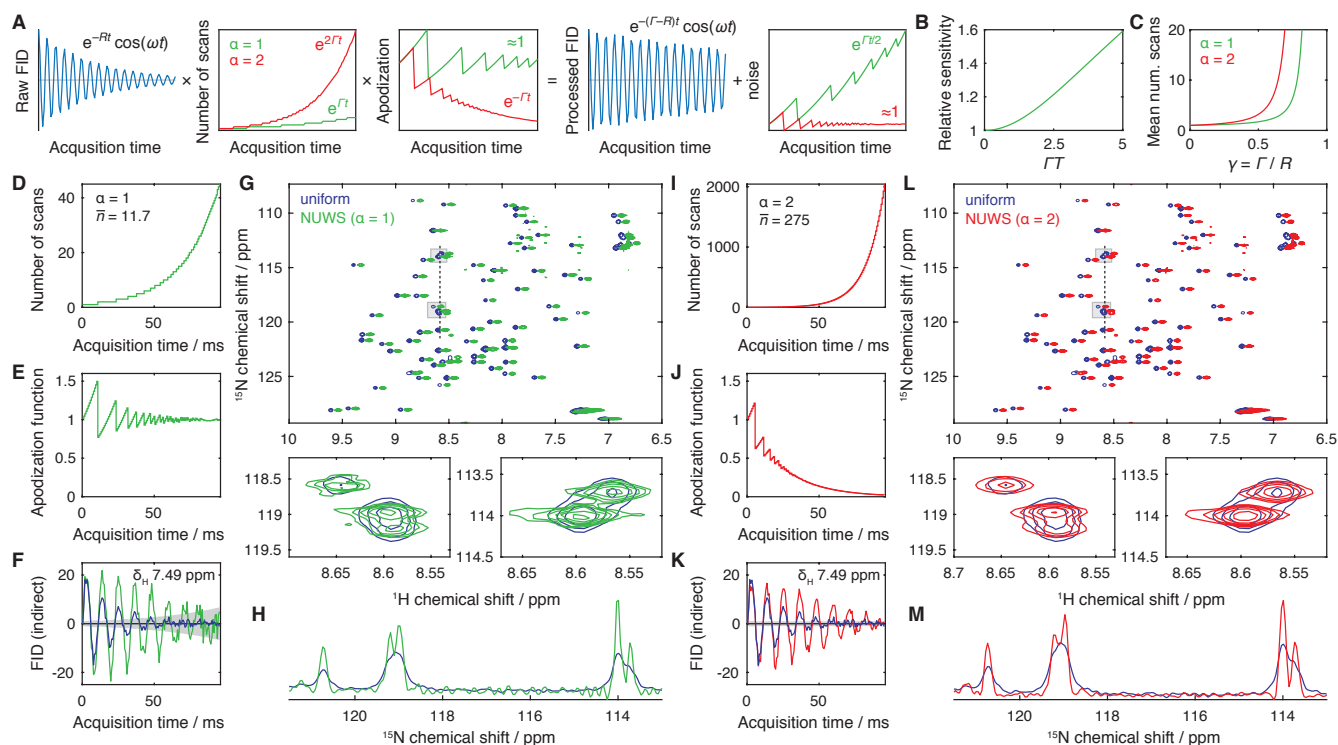


Figure 1. Resolution enhancement using non-uniform weighted sampling. (A) Schematic illustration of acquisition scheme for the application of a resolution enhancing window function, $w(t) = e^{\Gamma t}$, via the sampling weights $n(t) = e^{\Gamma t}$ (green) and $e^{2\Gamma t}$ (red), and apodization functions $h(t) = w(t)/n(t)$. $R = 25 \text{ s}^{-1}$, $\Gamma = 20 \text{ s}^{-1}$, $\omega = 1000 \text{ s}^{-1}$ and $T_{\text{aq}} = 100 \text{ ms}$. (B) Relative sensitivity of acquisition with $\alpha = 1$ (sensitivity optimised NUWS) vs $\alpha = 0$ or 2 (uniform sampling or constant noise NUWS) (Eq. 6). (C) Mean number of scans required for acquiring spectra with a fold reduction in linewidth $R/(R - \Gamma)$, and acquisition time $T = 1/(R - \Gamma)$, relative to uniform sampling (Eq. 7). (D–M) Resolution enhancement of ^1H , ^{15}N -SOFAST-HMQC spectra of ubiquitin (277 K, 600 MHz) acquired using (D–H) maximum sensitivity ($\alpha = 1$, green) and (I–M) constant noise ($\alpha = 2$, red) weighted sampling schemes. (D, I) Sampling weights and (E, J) apodization functions for 40 s^{-1} (13 Hz) resolution enhancement with a 96 ms acquisition time. The average number of scans, \bar{n} , is indicated. (F, K) ^{15}N time domain signals (real part) measured for the R54 resonance using (blue) uniform sampling and (green/red) non-uniform weighted sampling schemes. The noise level at each time point in indicated with grey shading. (G, L) ^1H , ^{15}N -SOFAST-HMQC spectra acquired with uniform sampling (blue) and NUWS resolution enhancement (green/red, shown with a 0.08 ppm ^1H offset for clarity). Magnified plots of the boxed regions are shown underneath. Contour levels are normalized according to the number of scans in the first increment. (H, M) ^{15}N cross-sections, marked with a dashed line in panels G and L.

In addition to this sensitivity-optimised sampling scheme ($\alpha = 1$), we have also identified a second NUWS scheme of interest. In this case, $\alpha = 2$ (Fig. 1A, red), additional scans are acquired, such that when re-scaled by the apodization function $h(t) \approx e^{-\Gamma t}$ the noise level remains constant (except for small deviations arising from integer sampling weights). Resolution enhanced FIDs obtained using this scheme are therefore truly free of artefacts. While the sensitivity per unit time of this approach is identical to uniform sampling ($\alpha = 0$, Eq. 5), the disadvantage of this scheme is the increased acquisition required to accumulate the larger number of scans at later time points. However, the effectively perfect resolution enhancement and uniform noise obtained using this NUWS scheme may be used in conjunction with sparse non-uniform sampling (NUS) and reconstruction to reduce the overall acquisition time. It would also be possible to apply a second apodization function, e.g. cosine or cosine squared, to the resolution-enhanced FID using NUWS methods, in which case the time consuming acquisition of late points

would be avoided. However, this approach would prevent extrapolation of the FID using linear prediction or other methods. As this seems counter-productive to the main goal of resolution enhancement, we have not explored this possibility further.

It is helpful to estimate the additional acquisition time required for a useful degree of resolution enhancement. When the relaxation rate of the signal is decreased, longer acquisition times are required to benefit from this enhanced resolution, such that $T \approx 1/(R - \Gamma)$. The average number of scans (Eq. 4) may then be expressed as a function of the relative reduction in linewidth, $R/(\Gamma - R)$:

$$\bar{n} = \left(e^{\frac{\alpha\Gamma}{R-\Gamma}} - 1 \right) \frac{R - \Gamma}{\alpha\Gamma} \quad (7)$$

This is plotted in Fig. 1C, for both optimal sensitivity ($\alpha = 1$) and constant noise ($\alpha = 2$) NUWS schemes. The function increases for large resolution enhancements, indicating a practical if not theoretical limit to the approach. Equally however, linewidths may be significantly reduced, by 4.6-fold or 2.8-fold ($\alpha = 1$ or 2 respectively), with a ten-fold increase in acquisition time, which is entirely practical when rapid longitudinal relaxation optimised SOFAST or BEST experiments are employed^{15–17}.

To test our approach experimentally, we acquired ^1H , ^{15}N SOFAST-HMQC spectra¹⁵ of ubiquitin (277 K, 600 MHz), using uniform sampling, or applying 40 s^{-1} resolution enhancement with both optimal sensitivity ($\alpha = 1$) and constant noise ($\alpha = 2$) NUWS schemes (Fig. 1D–M). We note that in contrast to hard pulse HMQC experiments, the use of amide-selective pulses in the SOFAST-HMQC means that scalar couplings to $\text{H}\alpha$ atoms are refocused in the indirect dimension. These experiments are therefore an attractive target for further resolution enhancement.

Sampling and apodization schemes are shown in Fig. 1D, E, I and J. Spectra were acquired using a minimal phase cycle for the first point, and total acquisition times were 2.6 min, 30 min and 9.5 hr for uniform, $\alpha = 1$ and $\alpha = 2$ NUWS schemes respectively. Both NUWS schemes worked effectively, and the increase in spectral resolution is easy to identify (Fig. 1G,H,L,M). Moreover, the impact of exponentially increasing noise on the spectrum in the sensitivity-optimised case (Fig. 1G,H) is limited, indicating that this reasonably rapid acquisition scheme may be of practical utility for a variety of common measurements.

In the second part of this paper, we consider the use of NUWS to decouple multiplets typically observed for uniformly ^{13}C -labelled proteins due to the evolution of homonuclear $^1J_{\text{CC}}$ scalar couplings during indirect chemical shift evolution periods. Such couplings give rise to signal modulations of the form $\cos^n(\pi Jt)$, where n is the number of coupled spins. Here we will focus on the case of terminal methyl groups, for which $n = 1$. Fortunately, aliphatic $^1J_{\text{CC}}$ coupling constants are generally similar in magnitude, ranging between 32 and 40 Hz¹¹. Therefore, we employ a similar strategy to above, and seek to apply a constant noise NUWS scheme to remove the $\cos(\pi Jt)$ modulation from the observed signal. However, a complication arises that was not present above: the zero crossings of $\cos(\pi Jt)$ at $1/(2J)$, $3/(2J)$, etc. result in singularities in the required sampling schedule, $n(t) = [\sec^2(\pi Jt)]$. The solution we propose here is to omit all measurements in the vicinity of these points, and subsequently use NUS reconstruction methods to fill in the gaps in the acquired FIDs (Fig. 2). Although not randomly sampled, the low degree of sparsity nevertheless allows effective reconstructions to be obtained.

To demonstrate this approach experimentally, we have acquired ^1H , ^{13}C methyl-SOFAST-HMQC spectra¹⁶ of uniformly ^{13}C -labelled ubiquitin (277 K, 600 MHz). A sampling schedule was prepared based on a 35 Hz $^1J_{\text{CC}}$ coupling constant, with a 40 ms acquisition time (Fig. 3A). 7 complex points were omitted either side of the zero crossing at 14.3 ms, resulting in 12% sparsity and a mean sampling density $\bar{n} = 2.8$. The number of skipped points was chosen empirically: when too many points were omitted the quality of NUS reconstruction was reduced, while when fewer points were omitted small differences in intensity due to variations in J couplings were amplified by the large number of scans required near the zero crossing, again resulting in artefacts. In practical terms, an increased

number of skipped points also resulted in a reduced acquisition time (lower \bar{n}).

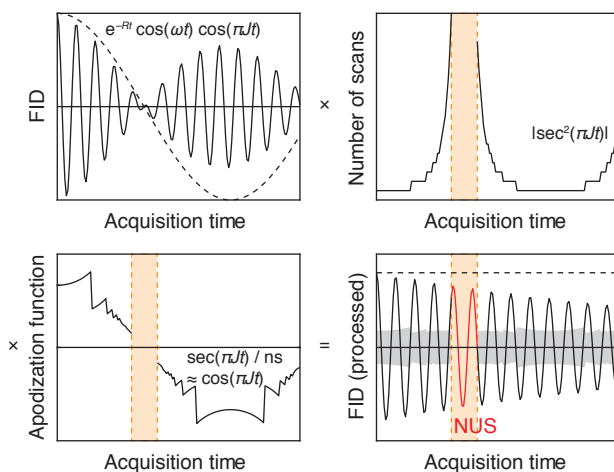


Figure 2. Homonuclear decoupling using NUWS and NUS reconstruction. The acquisition and processing of a J -modulated FID is illustrated, wherein points close to the zero crossing ($t = 1/(2J)$, $3/(2J)$ etc.) are omitted (orange shading) and reconstructed using NUS methods. The noise level at each point in the final FID is shown with grey shading.

Uniformly sampled and NUWS experiments were acquired using the sampling, apodization and NUS scheme in Fig. 3A, and representative FIDs are shown in Fig. 3B. The phase inversion following the zero crossing can be clearly observed in the NUWS signal, resulting from application of a negative apodization function (Fig. 3A). NUS reconstruction was performed using SMILE¹⁹ (Fig. 3B, red) and the final 2D spectra are plotted in Fig. 3C, together with a constant-time HSQC for reference (constant-time period $2T = 53.2$ ms).

The $^1J_{CC}$ coupling can clearly be observed in the uniformly sampled HMQC spectrum (Fig. 3C, blue), while decoupled singlets are observed in both the NUWS-NUS decoupled spectrum (Fig. 3C, red) and the CT-HSQC (Fig. 3C, green). The quality of the reconstruction is high, and examination of one-dimensional cross-sections (Fig. 3D) again shows that effective decoupling has been achieved, resulting in significantly more intense singlet resonances. In contrast to the CT-HSQC, the natural line width of signals is retained, i.e. FIDs decay as e^{-Rt} rather than being scaled by the amplitude e^{-2RT} , where $2T = 53.2$ ms is the duration of the constant time period. As a result, resonances are not only more intense but also more uniform using the NUWS-NUS decoupling approach, in contrast to the CT-HSQC for which fast-relaxing spins can be hard to detect.

We note that multiple coupling multiplicities cannot be decoupled simultaneously using NUWS-NUS, unlike CT experiments, as separate sampling schedules are required for each pattern of scalar coupling evolution. However, because these different types of spin systems are generally in well separated regions of the spectrum, and analyses often focus on only one subgroup of signals, such as methyl groups (excluding methionine C ϵ , which do not have $^1J_{CC}$ couplings), in practical situations this requirement may not be overly restrictive. Moreover, as acquisition is rapid relative to insensitive CT-HSQC experiments, multiple sampling schemes may be acquired in separate experiments if required.

In summary, we have demonstrated that NUWS may be used to enhance the resolution of multidimensional NMR experiments, and have shown how signals may be oversampled and apodized in order to modulate their envelopes in an arbitrary manner while maintaining a uniform noise level. This has opened up the possibility of further signal manipulations such as non-uniform sampling and reconstruction, and we have used this approach to develop a simple NUWS-NUS homonuclear decoupling technique. A number of applications may be envisaged for these methods, for example: increasing the spectral resolution for high molecular weight molecules, where perdeuteration

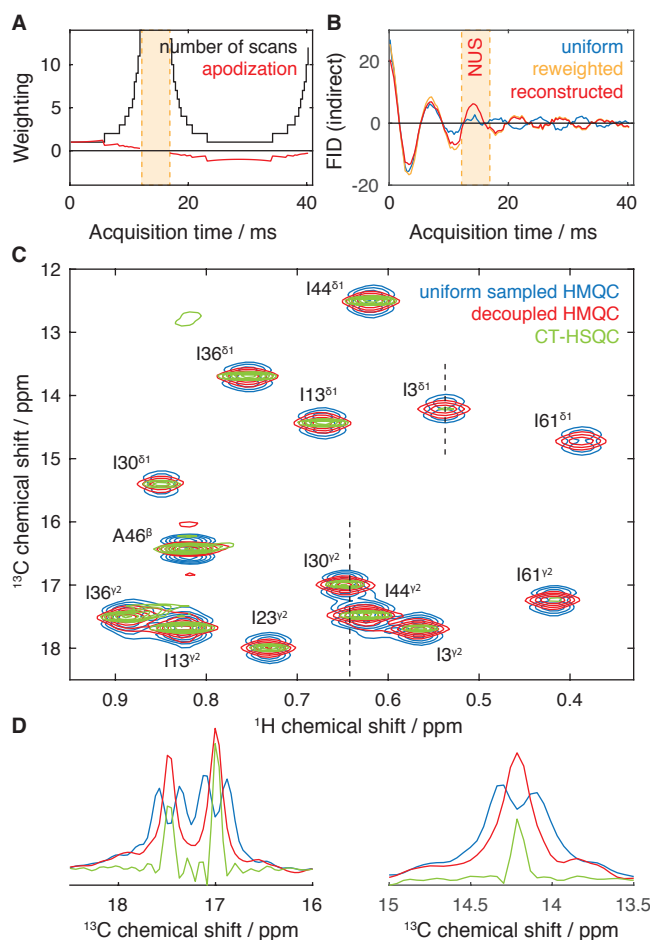


Figure 3. Homonuclear decoupling of a ^1H , ^{13}C SOFAST-HMQC spectrum¹⁶ of ^{13}C , ^{15}N -labelled ubiquitin (277 K, 600 MHz) using NUWS and NUS reconstruction. (A) Weighted sampling scheme and apodization function used for acquisition. Points omitted for NUS reconstruction are indicated with orange shading. (B) ^{13}C time domain signals (real part) acquired for the L50 $^{\delta 2}$ resonance (-0.23 ^1H ppm) using uniform or non-uniform weighted sampling, with NUS reconstruction using SMILE¹⁹. (C) ^1H , ^{13}C SOFAST-HMQC spectra¹⁶ of ubiquitin acquired with uniform weighting (blue), and decoupled following NUWS acquisition and NUS reconstruction (red). Contour levels are normalised according to the number of scans in the first increment. A constant time HSQC spectrum (53.2 ms constant time period) is shown for comparison (green). Assignments from bmrB entry 6457. (D) ^{13}C cross-sections indicated by dashed lines for the spectra shown in (C).

is either not sufficient, or not available, for example in mammalian expressed proteins²⁰, or studies at natural isotopic abundance²¹; increasing the accuracy of frequency-based measurements of residual dipolar couplings; combination with homonuclear decoupling in the direct dimension and/or NUS or spectral aliasing to obtain ultra high-resolution 2D measurements^{2,22}; sensitive and high-resolution analyses of the interactions of side-chains through titration experiments using uniformly ^{13}C -labelled material; and as a simple approach to decouple $C\alpha$ - $C\beta$ scalar couplings in HNCA and other 3D experiments.

Acknowledgements

We acknowledge the use of the UCL Biomolecular NMR Centre and the staff for their support. This work was supported by the Francis Crick Institute through provision of access to the MRC Biomedical NMR Centre. The

Francis Crick Institute receives its core funding from Cancer Research UK (FC001029), the UK Medical Research Council (FC001029), and the Wellcome Trust (FC001029). This work was supported by a Wellcome Trust Investigator Award (to J.C., 206409/Z/17/Z) and the BBSRC (BB/T002603/1).

Additional information

Experimental Procedures. Listing S1: Implementation of NUWS in Bruker format pulse programs. Listing S2: Python script for generation of vclist sampling schedules. Listing S3: Python script for apodization of NUWS data.

Competing interests The authors declare no competing financial interests.

References

1. Banci, L. *et al.* Biomolecular NMR at 1.2 GHz. *arXiv* (2019). [1910.07462v1](https://arxiv.org/abs/1910.07462v1).
2. Marcó, N., Fredi, A. & Parella, T. Ultra high-resolution HSQC: application to the efficient and accurate measurement of heteronuclear coupling constants. *Chem. Commun. (Camb.)* **51**, 3262–3265 (2015).
3. Rovnyak, D., Hoch, J. C., Stern, A. S. & Wagner, G. Resolution and sensitivity of high field nuclear magnetic resonance spectroscopy. *J. Biomol. NMR* **30**, 1–10 (2004).
4. Kerfah, R., Plevin, M. J., Sounier, R., Gans, P. & Boisbouvier, J. Methyl-specific isotopic labeling: a molecular tool box for solution NMR studies of large proteins. *Curr. Opin. Struct. Biol.* **32**, 113–122 (2015).
5. Pervushin, K., Riek, R., Wider, G. & Wüthrich, K. Attenuated T2 relaxation by mutual cancellation of dipole-dipole coupling and chemical shift anisotropy indicates an avenue to NMR structures of very large biological macromolecules in solution. *Proc. Natl. Acad. Sci. U.S.A.* **94**, 12366–12371 (1997).
6. Tugarinov, V., Hwang, P. M., Ollershaw, J. E. & Kay, L. E. Cross-correlated relaxation enhanced ^1H [bond] ^{13}C NMR spectroscopy of methyl groups in very high molecular weight proteins and protein complexes. *J. Am. Chem. Soc.* **125**, 10420–10428 (2003).
7. Robson, S. A. *et al.* Mixed pyruvate labeling enables backbone resonance assignment of large proteins using a single experiment. *Nat Commun* **9**, 356–11 (2018).
8. Ohki, S. y. & Kainosho, M. Stable isotope labeling methods for protein NMR spectroscopy. *Prog Nucl Magn Reson. Spectrosc* **53**, 208–226 (2008).
9. Coote, P. W. *et al.* Optimal control theory enables homonuclear decoupling without Bloch-Siegert shifts in NMR spectroscopy. *Nat Commun* **9**, 3014–9 (2018).
10. Shimba, N., Stern, A. S., Craik, C. S., Hoch, J. C. & Dötsch, V. Elimination of ^{13}C alpha splitting in protein NMR spectra by deconvolution with maximum entropy reconstruction. *J. Am. Chem. Soc.* **125**, 2382–2383 (2003).
11. Vuister, G. W. & Bax, A. Resolution enhancement and spectral editing of uniformly ^{13}C -enriched proteins by homonuclear broadband ^{13}C decoupling. *J. Magn. Reson.* **98**, 428–435 (1992).
12. Kumar, A., Brown, S. C., Donlan, M. E., Meier, B. U. & Jeffs, P. W. Optimization of two-dimensional NMR by matched accumulation. *J. Magn. Reson. (1969)* **95**, 1–9 (1991).
13. Waudby, C. A. & Christodoulou, J. An analysis of NMR sensitivity enhancements obtained using non-uniform weighted sampling, and the application to protein NMR. *J. Magn. Reson.* **219**, 46–52 (2012).
14. Simon, B. & Köstler, H. Improving the sensitivity of FT-NMR spectroscopy by apodization weighted sampling. *J. Biomol. NMR* **73**, 155–165 (2019).

15. Schanda, P. & Brutscher, B. Very fast two-dimensional NMR spectroscopy for real-time investigation of dynamic events in proteins on the time scale of seconds. *J. Am. Chem. Soc.* **127**, 8014–8015 (2005).
16. Amero, C. *et al.* Fast two-dimensional NMR spectroscopy of high molecular weight protein assemblies. *J. Am. Chem. Soc.* **131**, 3448–3449 (2009).
17. Favier, A. & Brutscher, B. Recovering lost magnetization: polarization enhancement in biomolecular NMR. *J. Biomol. NMR* **49**, 9–15 (2011).
18. Deckert, A. *et al.* Structural characterization of the interaction of α -synuclein nascent chains with the ribosomal surface and trigger factor. *Proc. Natl. Acad. Sci. U.S.A.* **113**, 5012–5017 (2016).
19. Ying, J., Delaglio, F., Torchia, D. A. & Bax, A. Sparse multidimensional iterative lineshape-enhanced (SMILE) reconstruction of both non-uniformly sampled and conventional NMR data. *J. Biomol. NMR* **68**, 101–118 (2017).
20. Sastry, M., Bewley, C. A. & Kwong, P. D. Effective isotope labeling of proteins in a mammalian expression system. *Meth. Enzym.* **565**, 289–307 (2015).
21. Arbogast, L. W., Brinson, R. G. & Marino, J. P. Mapping monoclonal antibody structure by 2D ^{13}C NMR at natural abundance. *Anal. Chem.* **87**, 3556–3561 (2015).
22. Kiraly, P. *et al.* Real-time pure shift ^{15}N HSQC of proteins: a real improvement in resolution and sensitivity. *J. Biomol. NMR* **62**, 43–52 (2015).